Electroluminescent Quantum Dots (ELQD) Performance Modeling

CORNING

Issued: August 2021
Supercedes: May 2021

M. Mlejnek, S. Han, M. Xun
Corning Incoporated, Corning, N.Y.

M. Kanehiro, Y. Nakanishi, Y.Koyama, and T. Ishida
Sharp Display Technology Corporation, Japan

This paper was presented at SID Display Week 2021.

Abstract

An optimized top emitting (TE) electroluminescent quantum dot (ELQD) LED device design is achieved using Finite Difference Time Domain (FDTD) simulation by allowing the thicknesses for QD Emission layer (EML) and an adjacent hole transmission layer (HTL) to differ for R, G, and B subpixels. Optical extraction efficiencies for R, G, and B subpixels reach ~15, ~23, and ~24 % resp., while small angular color shift is sustained. Angular characteristics of the device are very sensitive to the thickness variation of the individual material layers in the design, indicating the importance of thickness control in device fabrication process.

I. Introduction

Organic LED (OLED) display market has been growing rapidly in recent years due to its high-quality image (true black, high contrast and wide viewing angles) and thin form factor, enabling bendable display products from foldable phones to rollable TV. Major disadvantages of OLED are screen burn-in and high manufacturing cost. Electroluminescent quantum dot (ELQD) offers an attractive alternative to OLED because it can deliver a large color gamut and a low-cost manufacturing. Large color gamut comes from the narrow emission spectrum of QD materials and low-cost manufacturing is made possible by the compatibility of QD materials to solution process such as ink-jet printing process.

As typical with early stage product development, there are still many issues to be solved with ELQD device, particularly in reliability and lifetime. These issues require integrated solution of materials, stack design and device reliability, which involves multiple factors and often performance trade-offs. Stack level optical modeling can be an ideal tool for design optimization.

For example, optical modeling can:

- Screen materials based on interlayer comparabilities
- Determine attributes and dimensional requirements
- Explore light extraction designs to max device performance

Collaborating with Sharp, Corning developed stack modeling capabilities that can be used to evaluate the impact of stack designs and materials on light coupling efficiency, color shift and brightness uniformity.

II. Method

Optical model was set up to simulate performance of ELQD device. Model inputs are thickness and refractive index of each layer in an ELQD stack. The performance metrics to be predicted by the model include optical efficiency (OE) and luminance angular distribution (LAD). OE is defined as the ratio of total optical energy emitted by the device to the energy generated by the dipole sources representing QDs and LAD informs us about energy distribution of the emitted light in the far-field.

Two types of emissive stack were simulated, i.e. bottom emission (BE) and top emission (TE) ELQD, as shown in Fig. 2.1. They are similar to the structures published in Ref. [1].

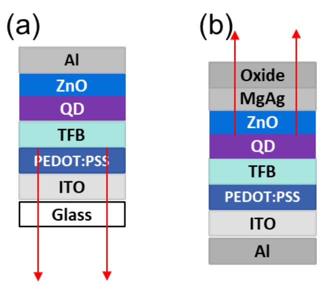

Figure 2.1. ELQD structure for (a) bottom emission and (b) top emission.

Electromagnetic power propagation in the stack was simulated numerically using the finite-difference-time-domain (FDTD) solver in Lumerical (Ansys) software, which solves Maxwell equations directly in a 3D geometry [2]. FDTD enables modeling of wide range of materials and geometries. Other numerical solvers, such as transfer matrix, can calculate optical OE and LAD in 2D layer stack more efficiently than FDTD. However, such solvers cannot deal effectively with complex refractive index of the layer where the dipole is located or with non-planar structures.

In FDTD simulation, photons generated by QD, via electroluminescence, were simulated as electromagnetic dipoles. The dipole is located inside EML (QD), but its exact location is not known. For initial validation, three dipole locations were simulated, i.e. closer to HTL, center of EML, and closer to ETL sites. Simulation were compared against experimental measurement to determine the best dipole location for simulation. For each dipole, its orientation is also not known and can be random. In order to get representative result, parallel and perpendicular dipoles were both simulated and probabilistically weighted results averaged over different dipole orientations were taken as the representative result for each location.

The simulation region includes all layers in the stack design and a glass or air region with thickness equal to half of the maximum wavelength for BE or TE structure, respectively. Outside the simulation region, perfect matching layer was used to reduce boundary reflection. Two detectors were set up to capture the total power emitted by the dipole and the electromagnetic field leaving the stack into the glass (BE) or air (TE). OE was calculated by taking the ratio of power leaving the stack to that emitted by dipole. OE was calculated as a function of wavelength and the total OE for QD emission is the average OE weighted by the emission spectrum of QD.

To calculate LAD, far-field projection of the near-field electromagnetic distribution was performed. In order to suppress diffraction artifact caused by the finite aperture size of near-field detector, data smoothing was applied in the projection. LADs at individual wavelengths were calculated first, then, by weighting them by the emission spectrum, the final ELQD device LAD was determined.

III. Model validation

We perform a validation study comparing model predictions to several measured device performance characteristics. In experiments, absolute values of OE are hard to extract due to the presence of electronic transport efficiency. Hence we compared quantitatively only LAD and color performance.

BE structure validation: We used BE to determine which dipole location better fits the experimental data. LAD at 540 nm for green BE ELQD device was measured and compared with simulation results for three different dipole orientation and their average. Simulation results for dipoles located closer to the TFB side show good match to measured results as shown in Fig 3.1. in agreement with expectations based on charge carrier transport. This conclusion was reinforced in the simulation/validation of the TE devices.

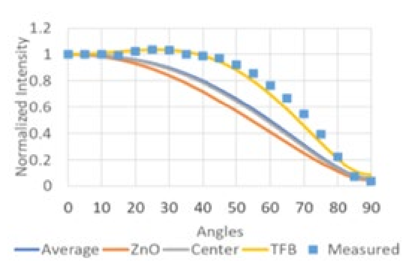

Figure 3.1. Validation of dipole position with experiment (Sharp's data).

TE structure validation: R/G/B ELQD devices with ITO anode thickness of 10 nm and 110 nm were fabricated. Simulated LADs were compared to measurements for those structures. The results are shown in Fig 3.2. Modeled and simulated LADs show good agreement for emission angles <50 degrees, except for one case. Investigation of this case is the focus of ongoing efforts; modeling can provide some insights by looking at the sensitivity of ELQD performance metrics to the variations in the individual layer thicknesses. We shall return to this issue in the next section. Larger discrepancy at higher emission angles can be attributed to measurement challenges due to low light signals and simulation inaccuracies. For example, the effect of (non-bonded) cover glass plate present in the experiment was accounted in modeling by including polarization averaged Fresnel effects [3].

For each device, color angular distribution and color shift was also calculated in u'-v' color coordinates and compared to measurement. There are noticeable discrepancies in the measured and simulated absolute color coordinate, which are currently not understood. However, the calculated angular color difference (Δu'-Δv') have similar trends and much better agreement, with experiment as can be seen in Fig. 3.3.

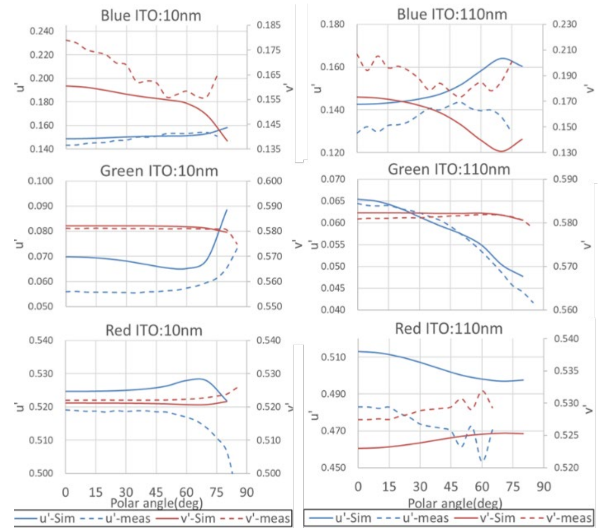

Figure 3.3 Measured (Sharp's data; dashed lines) and simulated (full lines) color angular distribution.

IV. Structure Optimization

We use maximum OE for all subpixels and good angular color balance as targets for ELQD structure optimization. Our bill of material was set (given by electronic charge transport optimization, or by customer Sharp; see Table 1 below), and since OE and LAD change with different thicknesses of the layers, we focused on TE ELQD performance evaluation as the layer thicknesses were varied.

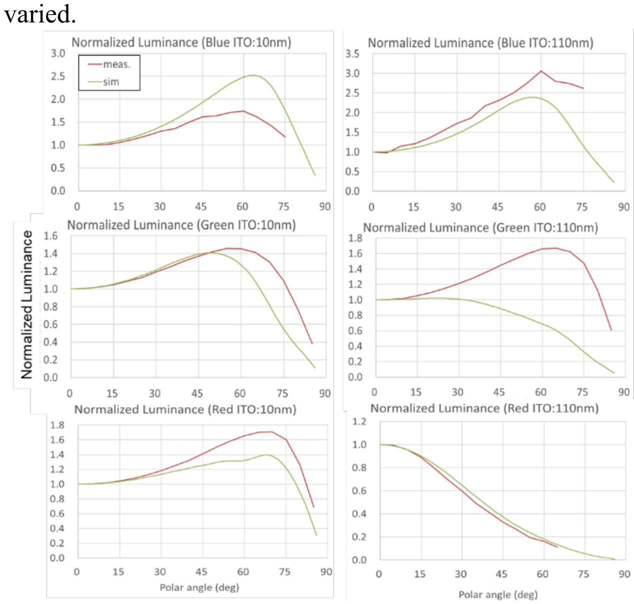

Figure 3.2. Measured (Sharp's data) (red) and simulated (blue – no cover glass; green – with cover glass) LAD.

***Single layer thickness optimization*:** Firstly, we studied OE and LAD changes while varying thickness of only one layer (either ITO or EML). When varying ITO thickness, keeping other layers at nominal values (30 nm EML, 35 nm HTL; for others see Table 1), we found that 150/110/70 nm thick ITO provides best OEs (>20%) for R/G/B subpixels, respectively.

Not considering ITO pixilation, we selected 110 nm thick ITO for all subpixels and searched for best ELQD performance as EML thicknesses were varied for different subpixels. The results are summarized in Fig. 4.1, where we can see that designs with very thin blue and relatively thick red EMLs could produce OEs only about ~10% for these subpixels (while green subpixel maintains > 20% OE). If we consider only uniform thickness changes of any of the layers, there is little room left for further improvement in red and blue subpixels simultaneously.

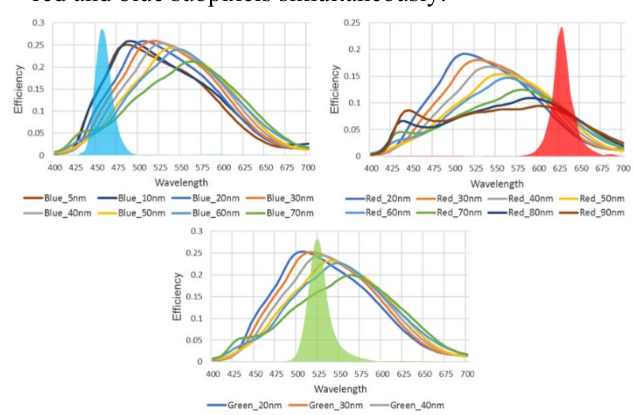

Figure 4.1. Simulated wavelength dependent OE of the three-color subpixels as a function of EML thickness (curves with corresponding legend in each picture). Here and later, QD emission power spectrum is shown in matching color. ITO thickness 110nm.

Additionally, LADs generated by different color subpixels are very different, leading to a large color shift as a function of emission angle. This is illustrated in Fig. 4.2, where we plot LADs for the same set of blue QD EML thicknesses as used in Fig. 4.1. Notice that the design with highest OE generates LAD with strongest emission to angles >30 deg, leading to LAD's donut shape, with lower luminance for smaller emission angles and higher luminance for intermediate emission angle range (Fig. 4.2 right). Such shape is not achieved for green or red subpixels, resulting in a high image color shift with observation angle.

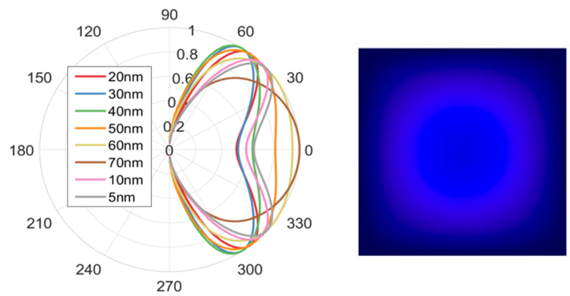

Figure 4.2. Left: Blue subpixel LADs for EML thicknesses ranging from 5 nm to 70 nm. On the right: True color plot for the case of 5 nm blue EML thickness.

To summarize, changing thickness of EML leads to designs with very thin blue QD EML and very thick red QD EML; this design has limited OEs and different LADs, resulting in large color shift.

Two layers' thicknesses optimization: Next, we optimized the structure when thicknesses of two constituent layers were varied. We chose EML(QD) and HTL(TFB), even though other pair of non-metallic layers could have been selected, we speculate, leading to only slightly different conclusions, since the indices of refraction of all the non-metallic layers are relatively close to each other.

Our simulations show that changing the thicknesses of two layers independently for the R/G/B subpixels leads to designs with much improved OE and LAD, resulting to acceptable color shift. Fig. 4.3 shows the improvement in OE as the EML and HTL thickness vary for red and blue subpixels (independently), as compared to the results presented in Fig. 4.1.

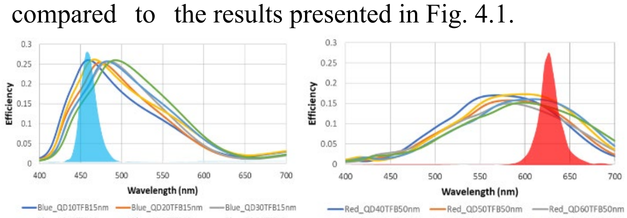

Figure 4.3. Wavelength dependent OE for the blue and red color subpixels, achieved by modifying EML and HTL thicknesses.

Furthermore, we observe that the LAD of the R/G/B subpixels can reach similar profiles without compromising OEs. We present parameters of a couple of designs with optimized OEs and LADs in Tables 1 & 2. LAD plots of one of the designs in Fig. 4.4 illustrates the degree of agreement of the LAD dependencies, from which color shift can be ascertained.

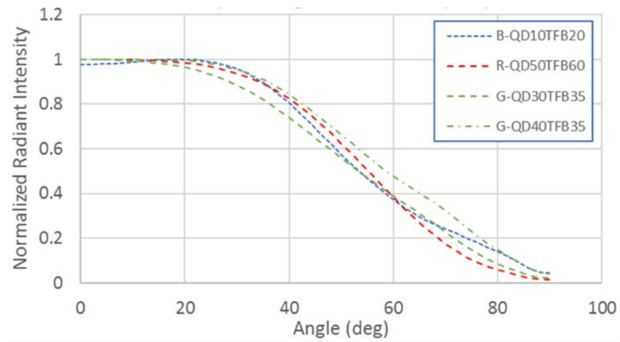

Figure 4.4. Device #1 optimized LAD for red, blue and two green subpixel candidates. Candidate shown as green dash-dot line was chosen for the device #1.

Table 1. Optimized two sets of TE ELQD prototypes. Nominal values highlighted in blue.

Layer	Material	Thickness (nm)	
		Device #1	Device #2
Top	Air	-	-
Cathode	Metal Oxide	20	20
	MgAg	15	15
ETL	ZnO	50	50
EML	QD (R/G/B)	50/40/10	40/20/10
HTL	TFB for (R/G/B)	60/35/20	60/35/15
HIL	PEDOT:PSS	40	40
Anode	ITO	110	110
Reflector	Ag	100	100

Table 2. Approximate OE for the optimized two sets of prototypes.

Layer	OE		
	R	G	B
Device #1	0.150	0.235	0.244
Device #2	0.149	0.231	0.237

As advertised in the previous section, modeling can provide means for evaluation of ELQD performance sensitivity to changes in individual or compound layer thicknesses. As an example, we report here on the modeled performance impact of ITO layer thickness change in the nominal design of device #1 (see Table 1), leaving the rest of the sensitivity study to another paper.

The LAD curves of the nominal design and designs with ITO thickness changed by +/-10 nm is shown in Fig 4.5. We can notice a strong dependence of LADs as a function of thickness variation, signifying a strong sensitivity of the designs to manufacturing tolerances. The results in Fig 4.5 suggest a mechanism that could explain observed discrepancy between measured and modeled LAD as discussed in the Model validation section.

V. Discussion and Conclusion

We have shown the progress in developing an optical modeling tool for emissive display device. For a given set of layer materials and stack structure, the tool can simulate the OE and LAD for R/G/B subpixels. Preliminary validation shows good match of modeled performance metrics to measured data. The tool was used to assist stack design, producing improved stacks with high OE and good angular color performance. A few insights learned from modeling on ELQD device: 1) multilayer pixilation is needed to get good color balance; 2) there is a flexibility in the designs that allows us to modify OEs of the R/G/B subpixels – typically trading of OE improvement of one subpixel as OE of another subpixel decreases – so the designs can be changed to fit the needs of the application; 3) device performance is very sensitive to layer thickness variation, therefore good process control is important to get the targeted device performance.

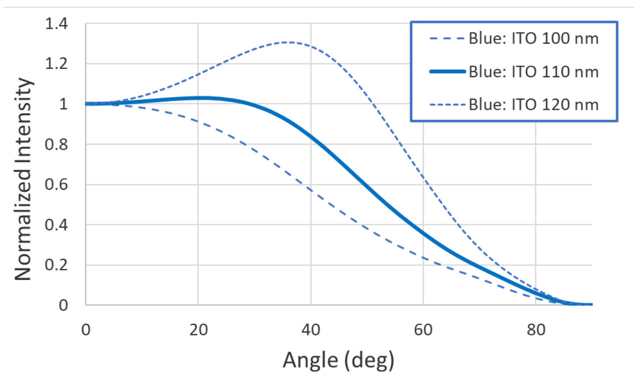

Figure 4.5. LAD for the blue subpixel as a function of EML, HTL, and ETL thickness deviations. Orange lines for EML, violet lines for ETL, and green lines for HTL. Thick blue line corresponds to the LAD of a blue subpixel device #1.

VI. Acknowledgements

We would like Corning-Japan Commercial team, in particular Yasuyuki Inoue, Hiroyuki Fukushima and Hiroyasu Suzuki, for facilitating the communications between Sharp Display Technology Corporation and Corning Incorporated. We also thank Hong Yoon and Fedor Kiselev for modeling discussions.

VII. References

1. Montgomery, D. J., Boardman, E.A., Dimmock, J.A.R., and Smeeton, T.M., "P-117 Simulation of Light Extraction from an Electroluminescent QD-LED." SID 2019 Digest, 1689 (2019).
2. Lumerical, FDTD, https://www.lumerical.com/
3. Fresnel, https://en.wikipedia.org/wiki/Fresnel_equations

This paper was published in the 2021 SID Digest .